Cancer Stem Cell Sorting from Colorectal Cancer Cell Lines by Sedimentation Field Flow Fractionation

ARTICLE *in* ANALYTICAL CHEMISTRY · FEBRUARY 2012

Impact Factor: 5.64 · DOI: 10.1021/ac202797z · Source: PubMed

7 AUTHORS, INCLUDING:

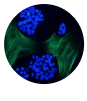

Carole Mélin
Université Libre de Bruxelles
10 PUBLICATIONS **67** CITATIONS
SEE PROFILE

Marie Jauberteau
University of Limoges
180 PUBLICATIONS **1,773** CITATIONS
SEE PROFILE

Philippe Jean Cardot
University of Limoges
77 PUBLICATIONS **1,216** CITATIONS
SEE PROFILE

Serge Battu
University of Limoges
78 PUBLICATIONS **819** CITATIONS
SEE PROFILE

analytical chemistry

Article

pubs.acs.org/ac

Cancer Stem Cell Sorting from Colorectal Cancer Cell Lines by Sedimentation Field Flow Fractionation

Carole Mélin,[†] Aurélie Perraud,[†,‡] Hussein Akil,[†] Marie-Odile Jauberteau,[†] Philippe Cardot,[†,§] Muriel Mathonnet,[†,‡] and Serge Battu*[,†,§]

[†]Institut 145 GEIST, EA 3842 "Homéostasie Cellulaire et Pathologies", Faculté de Médecine, Université de Limoges, 2 rue du Dr Marcland, 87025 Limoges Cedex, France

[‡]Service de Chirurgie Digestive Générale et Endocrinienne, Centre Hospitalier et Universitaire de Limoges, 2 rue Martin Luther King, 87042 Limoges Cedex, France

[§]Laboratoire de Chimie Analytique et Bromatologie, Faculté de Pharmacie, Université de Limoges, 87025 Limoges Cedex, France

ABSTRACT: Recently, cancer stem cells (CSCs) have been identified in many types of cancers, such as colorectal cancer (CRC). CSCs seem to be involved in initiation, growth, and tumor metastasis, as well as in radio- and chemotherapy failures. CSCs appears as new biological targets for cancer therapy, requiring the development of noninvasive cell sorting methods. In this study, we used sedimentation field flow fractionation (SdFFF) to prepare enriched populations of CSCs from eight cell lines corresponding to different CRC grades. On the basis of phenotypic and functional characterizations, "hyperlayer" elution resulted in a fraction overexpressing CSC markers (CD44, CD166, EpCAM) for all cell lines. CSCs were eluted in the last fraction for seven out of eight cell lines, but in the first for HCT116. These results suggest, according to the literature, that two different pools of CSCs exist, quiescent and activated, which can both be sorted by SdFFF. Moreover, according to CSC properties, enriched fractions are able to form colonies.

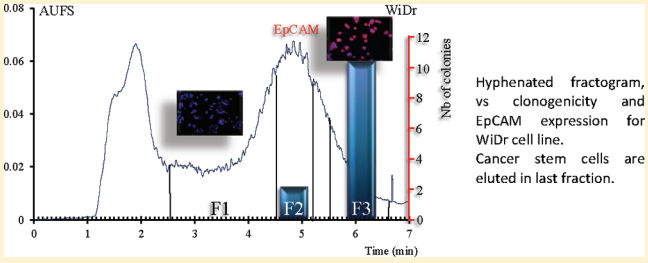

Colorectal cancer (CRC) is a leading cause of mortality in the Western world.[1] CRC is surgically curable in the early stages, whereas the tumor is not symptomatic until the metastatic stage associated with a high mortality. Despite the emergence of new targeted agents and the use of various therapeutic combinations, none of the treatment options available is curative in patients with advanced cancer. The mortality rate approaches 100% due to the propensity for early metastatic spread and because the disease is highly resistant to radiation and chemotherapy.[2] CRC development and therapeutic efficacy may be based on cancer stem cell (CSCs) existence.[1] CSCs or cancer-initiating tumor cells have been identified in several types of tumors, including CRC, through expression of specific markers associated with two other stem-cell-like properties: ability to self-renew and to generate mature cells.[3] CSCs can also give rise to heterogeneous tumors and are able to reproduce a tumor following transplantation in immunodeficient mice.[4] The CSCs hypothesis predicts that these subpopulations are responsible for driving growth[2] but also for therapy failures: cancer recurrence, emergence of resistant clones, and detrimental therapeutic escalation for the patient.[3] Phenotypic characterization of CSCs in CRC is still discussed. Initially, the CD133 protein was identified as a CSC marker,[5−7] but studies showed that $CD133^+$ expression is present in a large majority of tumor cells.[8] Alternatively, coexpression of different molecules presented as immature cell markers, such as CD44, CD166, and EpCAM, is now used to target a specific subpopulation.[9−13]

To study CSCs, major difficulties reside in the isolation and characterization of these potential biological targets, because of their low numbers. CSCs account for only a small fraction of tumor cells (<1−5%). Various techniques are available for cell separation and characterization such as fluorescent- or magnetic-activated cell sorting (FACS or MACS), which take advantage to specific antigen expression. However, for CSCs, phenotypic characterization is controversial and specific labeling necessary for these techniques can modify cells properties and induce cell differentiation. Development of methods to enrich CSCs without labeling is essential to avoid interference for further cell use. In this respect, methods based on intrinsic biophysical properties such as field flow fractionation (FFF) could be of great interest.[14] Sedimentation FFF (SdFFF) is a gentle, noninvasive, and tagless method.[15,16] These advantages are based on the drastic limitation of cell−solid-phase interactions by the use of (1) an empty ribbon-like channel without stationary phase and (2) the "hyperlayer" elution mode, a size/density-driven separation mechanism.[17−23] The principle of cell separation is based on physical criteria, such as size and density,[15−19,24] and depends on the differential

Received: October 24, 2011
Accepted: December 17, 2011
Published: December 17, 2011

elution of species submitted to the combined action of (1) a parabolic profile generated by flowing a mobile phase through the channel and (2) an external field applied perpendicularly to the flow direction.[19] In SdFFF, a multigravitational external field is generated by rotation of the separation channel in a rotor basket, constituting one of the most complex devices used in FFF separation.[19,24] In the past decade, we developed prototypes and applications for SdFFF cell sorting in many fields such as neurology, oncology, and stem cells.[24−32] Two aspects of SdFFF in oncology have been explored. The first concerns studies of chemical apoptosis or differentiation induction.[26,28,32−35] The second point concerns the isolation of specific phenotypes from the original crude population (culture cell lines, tumor fragments) in order to study phenotypic relationships, or for immature cancer cell sorting.[25,31] These previous results[25,29−31] led us to sort glioblastoma cancer stem cells.[27] SdFFF's ability to enrich CSC populations should be extended and validated for different cancer models such as CRC, with the further goal of therapeutic applications.

This study describes a strategy, based on SdFFF elution, to obtain CSCs subpopulations from complex populations of CRC cell lines. We used a wide panel of CRC cell lines classified from low to high tumor grade (pTNM stages for pathology tumor nodes metastases): Caco2, WiDr, HT-29, HCT116, SW480 (low grade, stage 2), DLD1, SW620 (intermediate grade, stage 3), and Colo205 (high grade, stage 4). Results of functional and phenotypic properties showed that SdFFF was able to sort enriched populations of immature cells having characteristics of CSCs.

EXPERIMENTAL SECTION

Cell Lines. The human CRC cells (Caco2, WiDr, HT-29, HCT116, SW480, DLD1, SW620, and Colo205) were obtained from American Type Culture Collection (ATCC, Manassas, VA, U.S.A.) and cultured according to their recommendations. Cells were incubated at 37 °C in a humidified 5% CO_2 environment and passaged at subconfluence. Cellular suspensions were obtained through trypsinization (0.5% trypsin for 5 min) and 1500 rpm centrifugation (5 min).

SdFFF Device and Cell Elution Conditions. The SdFFF separation device used in this study was previously described and schematized.[28,35] Channel dimensions were 818 mm × 12 mm × 0.175 mm with two 50 mm V-shaped ends with a measured total void volume of 1772 ± 6.00 μL (n > 6). The channel rotor axis distance was measured at r = 14.82 cm. Sedimentation fields were expressed in units of gravity, 1g = 980 cm/s^2, and calculated as previously described. Cleaning and decontamination procedures, control of rotation speed, as well as chromatographic and acquisition devices have been previously described.[28,35]

SdFFF elution of CRC cell suspensions (100 μL/2.5 × 10^6 cells/mL) resulted in the separation of four cell fractions collected and designated as follows: (1) Fn for fraction number with F1, F2, and F3 successively collected and (2) TP for total peak, collection started from the beginning of F1 to the end of F3. The mobile phase was sterile phosphate-buffered saline (PBS, pH 7.4) (Gibco BRL, Cergy-Pontoise, France). To obtain a sufficient quantity of cells for further biological and biophysical characterizations, successive SdFFF cumulative fraction collections were performed (3−15). Size measurement using a Coulter counter was performed as previously described.[28]

Relative Cell Metabolism Assay (MTT). Cells were seeded at 1 × 10^4 cells/well in a microtiter plate. After 24, 48, 72, and 96 h of incubation, MTT assays were performed according to the manufacturer's instruction (CellTiter96 Aqueous One solution, Promega, Madison, WI, U.S.A., G3582). Results were normalized using crude (= 1).

Cell Cycle Analysis. For DNA analysis, cells were fixed and permeabilized in 70% ice-cold ethanol at −20 °C overnight, washed in phosphate-buffered saline (PBS, pH 7.4), treated with RNase (40 U/μL, Boehringer, Reims, France), and stained with propidium iodide (PI; 50 μg/mL).

Immunofluorescence. Cells grown on 12 mm coverslips were rinsed twice in PBS, fixed with 4% paraformaldehyde (PFA) at room temperature for 20 min, and permeabilized or not with 0.1% Triton X-100. Nonspecific binding was blocked by a 30 min incubation with PBS−2% bovine serum albumin (BSA) at room temperature. Coverslips were then incubated overnight at 4 °C in blocking solution with the primary antibodies, CD44 (no. 3570, Cell Signaling, Beverly, MA, U.S.A.), EpCAM (no. 2929, Cell Signaling), CD166 (MAB6561, R&D systems, Minneapolis, MN, U.S.A.), and CK-20 (M7019, Dakocytomation, Glostrup, Denmark). Coverslips were incubated for 2 h at room temperature with Alexa Fluor 594 nm conjugated secondary antibodies diluted 1:5000 in PBS (goat antirabbit IgG Alexa Fluor 594 nm (A11012), goat antimouse IgG Alexa Fluor 594 nm (A11005) from Invitrogen, Grand Island, NY, U.S.A.). After three washes in PBS, nuclei were stained for 5 min with DAPI (4′,6-diamidino-2-phenylindole) (1:10000 in PBS). After intensive washes, coverslips were then inverted on slides and mounted with Dako fluorescent mounting medium (S3023, Dakocytomation). Negative controls were cells incubated with irrelevant normal mouse serum (Sigma-Aldrich, Saint-Quentin Fallavier, France) used at the same dilution as primary antibodies. Pictures were captured using a Leica microscope and a Leica digital camera. Images were processed using Leica IM500 Image Manager. To quantify positive cells for each marker, 3−5 fields were counted using Image J. The ratio of stained cells/number of total cells was calculated for each field to evaluate the percentage of positive cells. For EpCAM^{high} cells, which corresponded to cells having a higher fluorescence intensity compared to basal labeling, only very strongly stained cells were counted. Statistical analysis is described below.

Clonogenic Assays: Soft Agar Assay. Clonal agar culture was performed in a double-layer agar system: 1 mL of basal layer culture with a final 0.5% agar concentration was prepared in 35 mm^2 plastic Petri dishes. Then, 2.5 × 10^3 WiDr viable cells (triplicates) in 1 mL of upper layer medium (0.35% agarose) were overlaid on the preformed basal layer. Dishes were incubated for 30 days at 37 °C in a humidified 5% CO_2 environment. Only colonies visible to the naked eye were counted.

Matrigel 3D. For HCT116 cell line clonogenicity assays, 500 cells were placed in Matrigel growth-factor-reduced matrix (356231, BD Biosciences, Le Pont de Claix, France) in 12-well plates and covered with culture medium. Colonies were grown for 3 weeks at 37 °C in a humidified 5% CO_2 environment. Only colonies visible to the naked eye were counted.

Statistical Analysis. A statistical analysis of differences was carried out by analysis of variance (ANOVA) using StatView version 5.0 software (Abacus Concepts, SAS Institute Inc., Cary, NC, U.S.A.). P-values of less than 0.05 (Fisher's PLSD test) were considered to indicate significance.

dx.doi.org/10.1021/ac202797z | Anal. Chem. 2012, 84, 1549−1556

Table 1. Optimal Elution Conditions, Retention Ratio R_{obs}, Cell Diameter, and the Calculated Cell Elevation Value "s" of the Different CRC Cell Lines[a]

	elution conditions			diameter (μm)				
cell lines	field (g)	flow rate (mL/min)	R_{obs}	TP	F1	F3	radius (μm)	s (μm)
Caco2	15	0.8	0.522 ± 0.007	16.80	18.80	16.40	8.40	15.23
WiDr	8	0.8	0.459 ± 0.010	12.47	13.15	11.50	6.24	13.38
HT-29	10	0.9	0.518 ± 0.013	12.65	13.20	11.83	6.00	15.10
HCT116	20	0.8	0.411 ± 0.009	12.00	13.22	11.47	7.25	12.00
SW480	8	0.8	0.517 ± 0.010	13.22	13.96	13.34	6.61	15.08
DLD1	12	0.8	0.443 ± 0.016	14.50	15.30	12.91	6.33	12.92
SW620	8	0.8	0.488 ± 0.011	11.12	11.67	10.05	5.56	14.23
Colo205	8	0.8	0.437 ± 0.012	13.20	14.57	12.11	6.60	12.74

[a]Results are expressed as mean ± SD (n = 3 for size and n > 12 for R_{obs}). Cell diameter was measured by Coulter counter, and CRC cell lines are displayed by the mean of international TNM (tumor node metastasis) stage classification.

RESULTS AND DISCUSSION

SdFFF Elution of CRC Cell Lines. During the past decade, we have developed biocompatible SdFFF prototypes and cell sorting applications, in particular in the field of stem cells and oncology.[24−31] SdFFF is now considered as a mature macromethod for preparation of sterile and purified populations which respects (1) the functional integrity,[28,30−32,35] (2) short- and long-term viability without induction of apoptosis,[26,27,29,35] and (3) maturation and differentiation stages which are essential for undifferentiated cell sorting (stem cells and progenitors[25,27,29,31]). These properties are the consequence of both the limitation of harmful cell−cell and cell−surface interactions by using an empty channel and the absence of cell labeling (fluorescent or magnetic), which is of great importance when cell markers are not well-defined (in particular for stem cells), when commercial labels do not exist, or when they could interfere with further cell uses (culture, transplantation), or when they could induce differentiation (stem cells). To more reduce cell−surface interactions, and to enhance cell sorting, optimal elution conditions for each cell line (Table 1) should be selected for the biocompatible "hyperlayer" elution mode.[17−21,23,30,36] This focuses subpopulations in thin layers away from the accumulation wall, corresponding to their equilibrium position where the external field is exactly balanced by hydrodynamic forces.[17,19−21,23,24,36] This position only depends to cell biophysical properties, which are size and density as first-order parameters. Then "hyperlayer" elution order is size/density-dependent; large and less dense cells are focused in the faster streamlines to be eluted in first. As previously described,[28,30] the experimental retention ratio R_{obs} = void time versus retention time = t_0/t_R (measured by first-moment method)[23] was used to determine the different average velocity, retention order, and finally, the elution mode.

Representative fractograms and fraction collections of some CRC cell lines are displayed in Figure 1. For each cell line, we observed similar profiles with two major peaks, the first corresponding to unretained species (void volume peak, $R_{obs} \approx 1$), the second corresponding specifically to the cell population with $R_{obs} < 1$ (Table 1, Figure 1). As previously described,[17,18,24,32,33,36] "hyperlayer" mode was demonstrated by the means of field and flow rate dependence of R_{obs}. For example, R_{obs} for WiDr cells (0.459 ± 0.010, 8g, 0.8 mL/min) varied from 0.348 ± 0.013 (10g and 0.6 mL/min) to 0.520 ± 0.006 (8g and 1.2 mL/min). Similar results were obtained for other cell lines (data not shown). In the "hyperlayer" elution mode samples were lifted away from the accumulation wall, limiting harmful cell−surface interactions. By using the following equation[18]

$$s = \frac{R_{obs}\omega}{6} \quad (1)$$

in which ω is the channel thickness (175 μm), we calculated the value of s, the average distance from the center of the cell to the channel wall.[18] Under "hyperlayer" mode, s should be greater than particle radius r, calculated from the mean cell diameter. These results were obtained for all CRC cell lines studied (Table 1). Under "hyperlayer" mode, elution order was described to be, as first-order parameters, size- and density-dependent.[17−21,23] By measuring the mean diameter of cells eluted first (F1) and last (F3), we observed a decrease in diameter during elution for all CRC cell lines (Table 1) according to "hyperlayer" mode. However, if we compared HT29 and SW480, two cell lines with similar R_{obs} (≈ 0.517) and profiles, they did not have similar diameters, 12.65 and 13.20 μm, respectively, whereas cell diameter decreased between F1 and F3, ≈1.4 and ≈0.6 μm, respectively (Table 1). In this case, similar R_{obs} with different mean-sized species indicated that CRC cell line retention was also density-dependent as was predicted and demonstrated for "hyperlayer" cell elution.[26,28,32,33]

Then, as we described for different cell species, our results demonstrated that all the CRC cell lines were eluted under the "hyperlayer" mode.[24,25,27−30,32,33,35] After establishing conditions for "hyperlayer" elution of CRC cell lines, we had to demonstrate the ability of SdFFF to prepare enriched fractions of CSC.

Phenotypic Analysis. Putative CSC populations have been identified in several types of solid tumors, on the basis of the expression of specific markers and on stem-cell-like properties, corresponding, respectively, to phenotypic and functional characterizations. Phenotypic characterization of CSCs is still debated.[11] CD44, CD166, and EpCAM have recently been identified as surface markers associated with CSCs in several types of tumor such as CRC.[9−13] Coexpression of these molecules on tumor cells has been reported to identify the CSC pool more precisely than single-marker expression, and they were used to identify CSC fraction contents. Additionally, the colon differentiated cell marker, CK-20 (cytokeratin-20), was also assessed.

Marker expression was analyzed and quantified by indirect immunofluorescence (Figure 2). First of all, the expression level was studied according to CRC stage (Figure 2A). A higher CD44 expression level was observed in early stages such as

dx.doi.org/10.1021/ac202797z | Anal. Chem. 2012, 84, 1549−1556

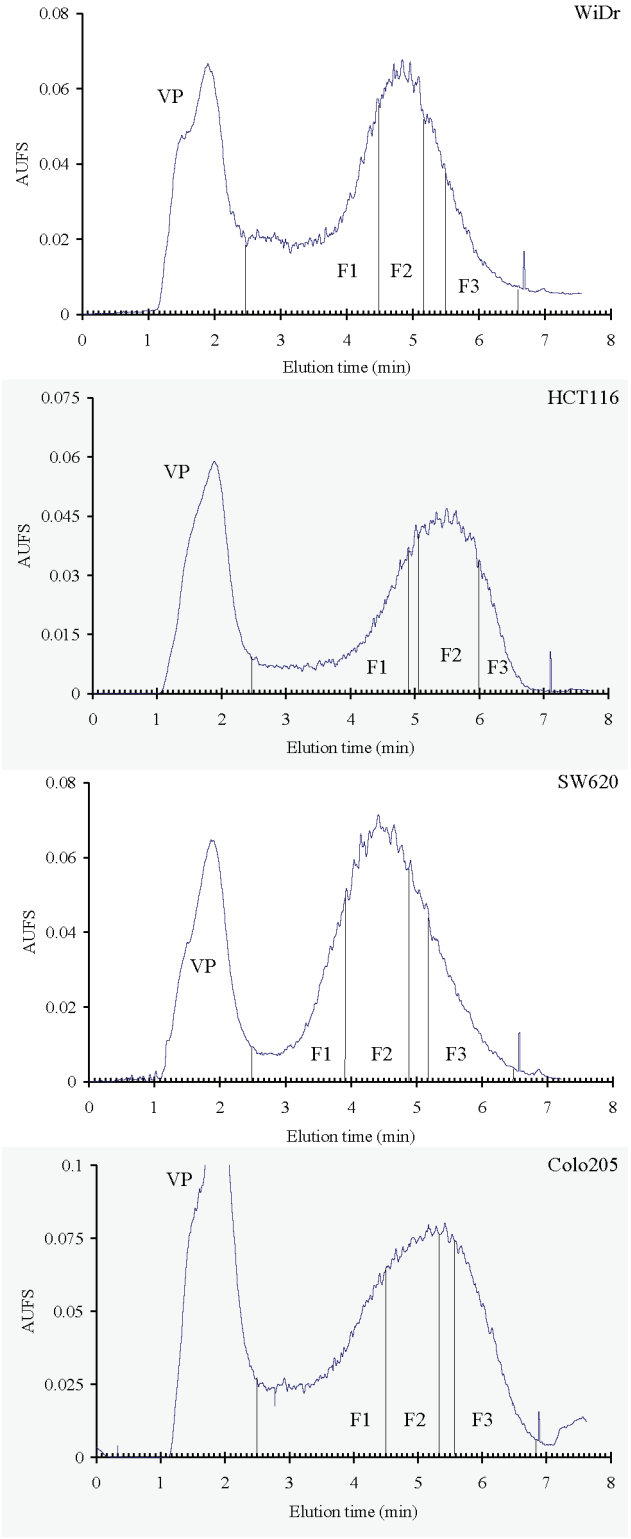

Figure 1. Representative fractograms of some CRC cell lines. Elution conditions: see Table 1. Fraction collections are indicated by vertical plain lines. TP = F1−F3. VP corresponds to the void peak.

Caco2, HT-29, and HCT116 (Figure 2A, part a). CD44 is a major adhesion molecule for the extracellular matrix[37] and has been implicated in a wide variety of physiological and pathological processes, including cell migration, tumor cell invasion, and metastasis.[38] We can hypothesize that CD44 decrease in advanced stages corresponds to loss of cell adhesion, a mechanism involved in metastasis. In contrast, CD166 expression was higher in advanced stages (Figure 2A, part b). CD166 (activated leukocyte cell adhesion molecule, ALCAM) expression is pathologically correlated with aggressive disease in a variety of cancers including CRC,[10] and overexpression seems to be correlated with shortened survival and aggressive tumor. Epithelial cell adhesion molecule (EpCAM) has been described as a dominant antigen in human CRC tissue: positive cells and expression level were increased in CSCs.[12] Basal and high ($EpCAM^{high}$) EpCAM expression did not appear to be associated with a specific stage (Figure 2A, parts c and d). Finally, CK-20 expression, a cytoskeleton protein expressed by more differentiated cells, rose in early stages (WiDr and HT-29) compared to advanced stages (Figure 2A, part e). In conclusion, expression patterns were different and agreed with specific cell lines and CRC stage.

After statistical evaluation, if no significant difference was observed between crude and TP fractions (data not shown), SdFFF significantly enriched a fraction with cells over-expressing one or more CSC markers. Intermediate stage cell lines, SW480 and DLD1, were characterized by an increase in only one CSC marker in F3: EpCAM and CD44, respectively (Figure 2A, parts a and c). Caco2, WiDr, HT-29, SW620, and Colo205 showed an increase in two or even three CSCs markers in F3 (Figure 2A). Basal EpCAM was overexpressed in F3 for lines corresponding to both low and high CRC grade. Moreover, compared to basal expression, $EpCAM^{high}$ cells were particularly increased in F3 for WiDr, HT-29, and SW620 (Figure 2A, part d, and 2B). Furthermore, WiDr, DLD1, and SW620 lines showed a decrease in $CK\text{-}20^{+}$ cells proportion in the F3.

Phenotypic characterization showed for seven out of eight cell lines that CSC was eluted in F3 with increased CSC marker expression. In contrast, the more differentiated cells, characterized by decreased expression of CSC markers and increased CK-20 expression, were eluted in F1. For HCT116 cells, we obtained the opposite result: all CSC markers were decreased in F3 as well as the number of $EpCAM^{high}$ cells (Figure 2B, parts e−h) while they were increased in F1. So, we suggested that CSCs from HCT116 cells were eluted in F1.

On the basis of phenotypic studies, results demonstrated that CSCs can be eluted using SdFFF. However, expression modulations of CSC markers contingent on cell lines, in particular for HCT116, led to functional studies to improve SdFFF CSC enrichment,

Functional Analysis. CSCs are supposed to have the same properties (stemness) as those of normal stem cells: reduced metabolism, cell cycle accumulation in G0/G1 phase which is linked to a more quiescent state, and also self-renewal.[9] To follow this study, we selected HCT116 and WiDr cells, two early CRC stages in which immature cells seem to be eluted in different fractions (F1 and F3, respectively).

First, the metabolic rate for each fraction was measured for 96 h (Figure 3). For WiDr cells, according to marker expression, F1 had a higher metabolic rate compared to the TP, F2, and particularly to F3. Significant differences were observed from 24 to 72 h of culture after SdFFF. Over these times, levels were similar between subpopulations (Figure 3A, 96 h) which suggests that culture conditions (FBS) could not preserve initial cell behavior over a long culture period. For HCT116, in contrast to WiDr, we observed a lower metabolism in F1 compared to F2 at 24 h which then remained constant (Figure 3B).

dx.doi.org/10.1021/ac202797z | Anal. Chem. 2012, 84, 1549−1556

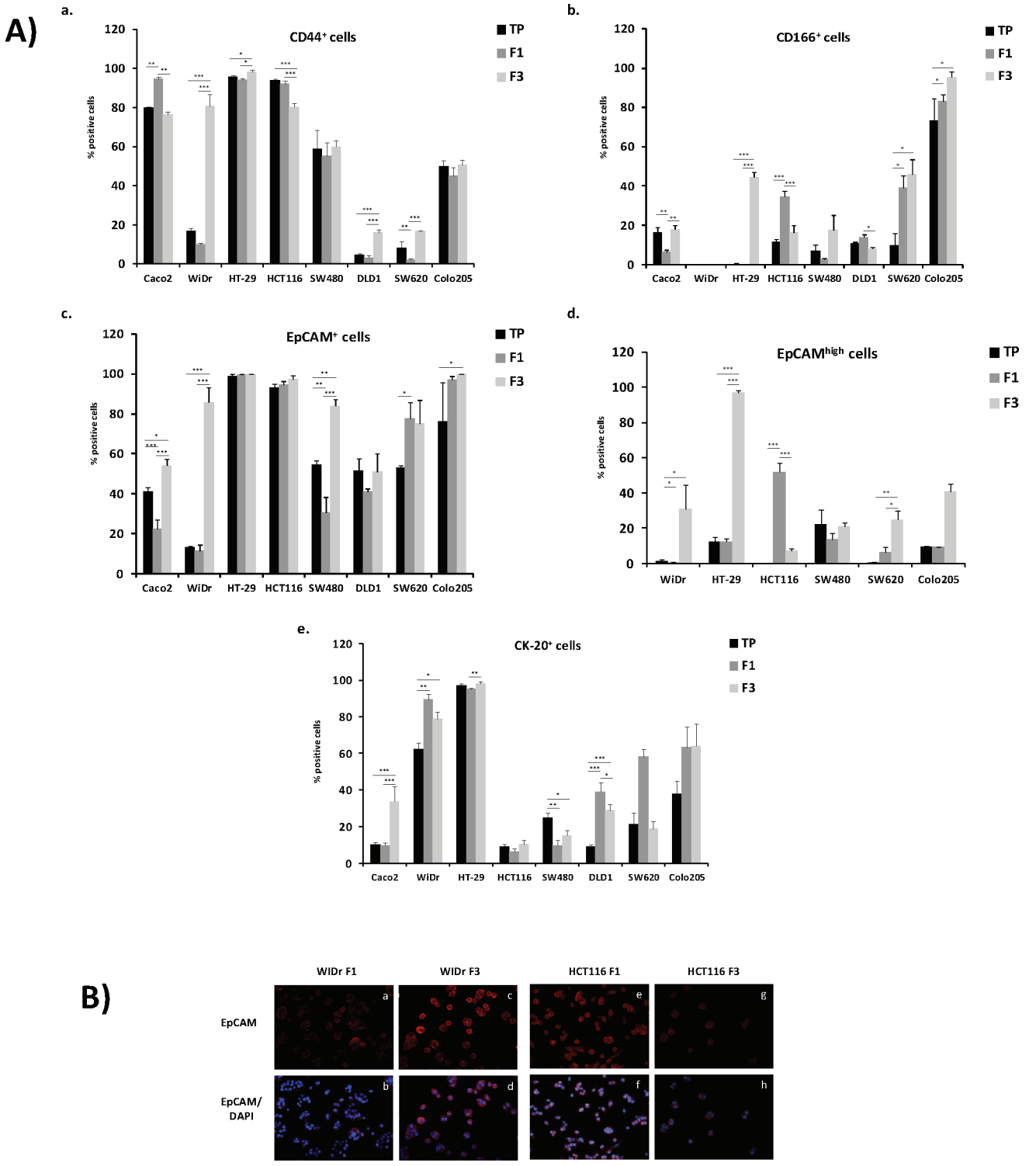

Figure 2. SdFFF-isolated subpopulation characterization by immunocytochemistry in cell lines using undifferentiated cell markers (CD44, CD166, and EpCAM) and a differentiated colon cell marker (CK-20). Protein expression was quantified and statistically analyzed (A) using StatView with an ANOVA test (* significant *p*-value): * $p < 0.05$; ** $p < 0.01$; *** $p < 0.001$. WiDr and HCT116 cells at 24 h of culture after SdFFF (B) by microscopy and immunofluorescence (magnification ×200). EpCAM labeling was done using Alexa Fluor 594 (red fluorescence) secondary antibodies, and labeled cells were counted using a nuclear marker (DAPI in blue).

For each cell line, cell cycle distribution showed no significant difference between crude and TP fractions, indicating that SdFFF cell sorting did not affect cell cycle distribution (Figure 4). For WiDr cells, the percentage of cells in G0/G1 was significantly higher in F3 ($P < 0.01$) than in F1 (1.5-fold over) (Figure 4A) which supported previous results.[28,30] WiDr F3 was enriched in less proliferative and quiescent cells, corresponding to CSC characteristics.[1] Similar to the metabolism assay, HCT116 F1 cells were not significantly enriched in proliferative cells with no significant increase in G2/M cells (Figure 4B). As with WiDr, a significant decrease of G2/M cells proportion was observed in F3.

dx.doi.org/10.1021/ac202797z | *Anal. Chem.* 2012, 84, 1549–1556

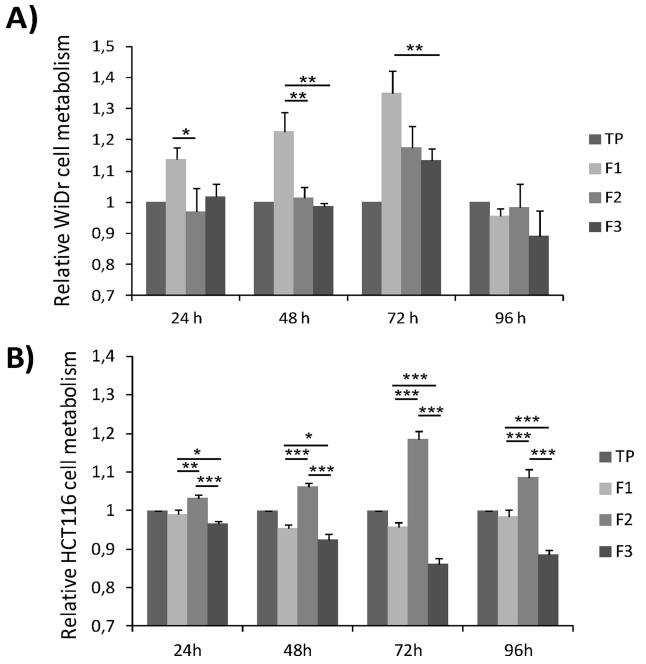

Figure 3. Relative cell metabolism after WiDr (A) and HCT116 (B) SdFFF elution sorting. Metabolic activity was determined by MTT assay and calculated relative to TP: * $p < 0.05$; ** $p < 0.01$; *** $p < 0.001$. No significant difference between crude and TP populations was observed.

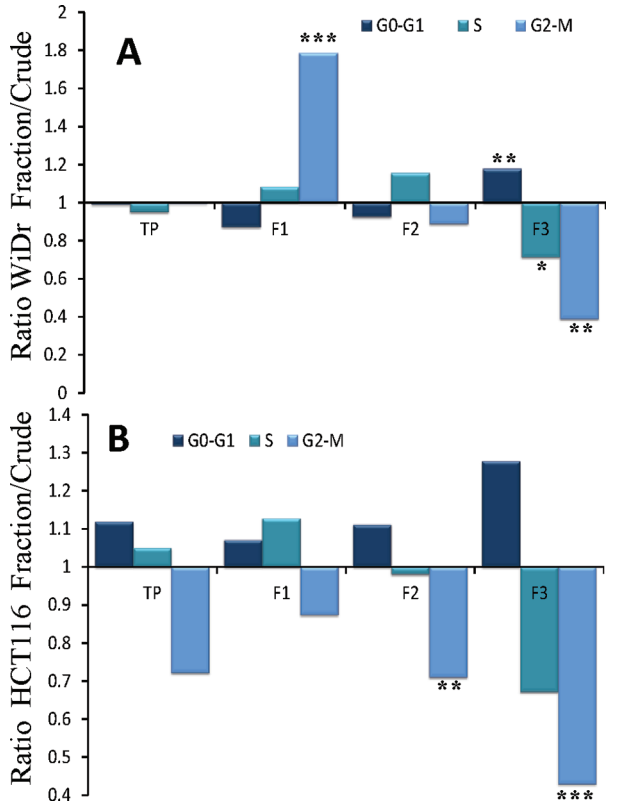

Figure 4. Cell cycle distribution in WiDr and HCT116 cell populations after SdFFF elution. Flow cytometry analyses indicated the number of cells in G0/G1 (nonproliferative state), S, and G2 (proliferative states) phases. Results are expressed as a ratio of the fraction compared to the crude population and statistically analyzed using StatView with an ANOVA test (* significant p-value) on WiDr (A) and HCT116 (B): * $p < 0.05$; ** $p < 0.01$; *** $p < 0.001$.

Taken together, MTT assay and cell cycle analysis showed that WiDr F3 cells behaved according to CSC characteristics (stemness[4]), as they corresponded to less proliferative and quiescent cells. As supposed, F1 HCT116 cells have a more original behavior. Compared to corresponding F1 WiDr cells, these cells were less proliferative and did not significantly accumulate in the S/G2/M part of cell cycle. Nevertheless, compared to F1, F3 HCT116 was the less proliferative and quiescent fraction, but they only expressed low levels of CSC markers. If a quiescent state is a normal stem cell property, this is not completely the case for F1 HCT116 cells. However, CSCs are responsible for driving tumor growth[2] and seem to be activated to give rise to heterogeneous tumors, which is not necessarily compatible with a quiescent state. Some studies have demonstrated that CSCs have similar properties to normal stem cells but have a higher proliferative capacity. Kuranda et al. recently showed that $CD34^+$ cells, corresponding to immature hematopoietic cells, proliferate more robustly compared to $CD34^-$ cells.[39] Further studies described the possible balance between quiescent and cycling states in CSCs, which could be explained as the difference between F1 HCT116 and F3 WiDr cells.[39,40] Nonetheless, SdFFF is able to separate cells regardless of their activation state: in WiDr, SdFFF is able to sort the least proliferating immature cells in F3, whereas in HCT116, activated CSCs are found in F1.

Finally, we studied the ability of these populations to self-renew, one of the most defining characteristics of stem cells. During cell division, one or both of the daughter cells remain undifferentiated.[9] CSCs are defined by similar properties, mainly their ability to self-renew, a characteristic that drives tumorigenesis and aberrant differentiation. Ability to form colonies matches with stem cell self-renewal capacity: one cell can expand and form a heterogeneous colony in vitro as well as a tumor in vivo. Clonogenic assays for WiDr fractions showed that few cells were able to form colonies in TP corresponding to the low CSC number in the crude population. This capacity was 6 times higher in F3, whereas no colonies were found in the F1 ($P < 0.001$, Figure 5A).

As no colony development was seen for HCT116 in agar–agarose assay, clonogenic assays were performed using Matrigel. In this line, CSCs seemed to be specifically restricted to F1, whereas nearly no colony was observed in other fractions ($P < 0.001$, Figure 5B). In accordance with phenotypic analysis, these results suggest that HCT116 immature cells sort early.

CONCLUSION

Colorectal cancer development and therapeutic efficacy may be based on the presence of cancer stem cells. CSCs are supposed to be responsible for driving growth, cancer recurrence, emergence of resistant clones, and detrimental therapeutic escalation for the patient, making them an important biological target for cancer therapies. To study CSCs, major difficulties remained (1) for isolation because of their low number (<1–5%) and (2) phenotypic characterization because of the definition of specific markers. Taken together, results of phenotypical (CD44, CD166, EPCAM, $EPCAM^{high}$, and CK-20) and functional (metabolism, cell cycle, clonogenicity) characterizations showed that SdFFF "hyperlayer" elution produced enriched fractions containing cells with CSC characteristics from all eight cell lines studied, corresponding to different CRC stages. For five of them, corresponding to the

dx.doi.org/10.1021/ac202797z | Anal. Chem. 2012, 84, 1549–1556

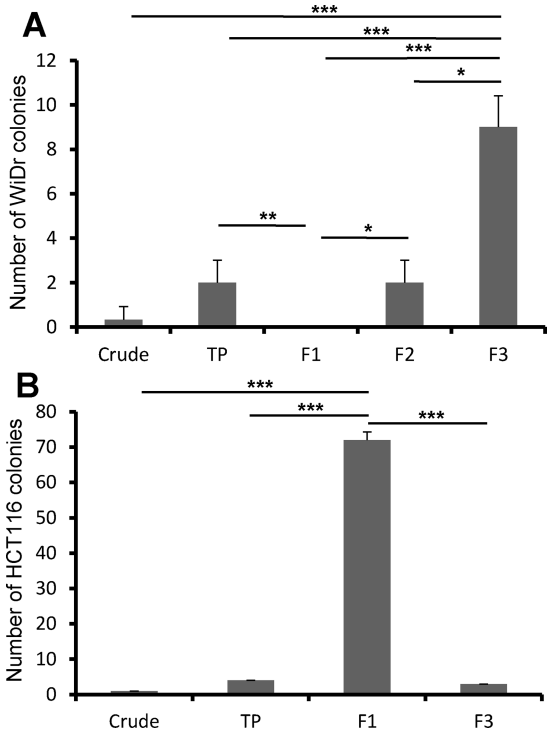

Figure 5. Clonogenic assay. Number of colonies was statistically analyzed for WiDr in soft agar assay (A) and HCT116 in Matrigel (B) using StatView with an ANOVA test (* significant *p*-value): * $p < 0.05$; ** $p < 0.01$; *** $p < 0.001$.

different CRC grades (HT-29, WiDr, HCT116, SW620, and Colo205), we observed a significant increase in CSC markers of around 10-fold or more. With the exception of the HCT116 cells, CSCs were eluted in the last fraction. As demonstrated for WiDr cells, they corresponded to less proliferative and more quiescent and clonogenic cells. Cells with CSC properties were eluted in F1 for HCT116. From a biological point of view, as supported by the recent literature, this suggests the existence of different CSC subpopulations according to activation state. Nevertheless, SdFFF is able to produce these different specific targets for further in vitro/in vivo characterization (ability to reinitiate tumors, radio- and chimio-resistance) as it seems important to focus research on new therapies to eradicate CSCs. The conditions for inducing differentiation of these immature cells or targeting them directly need to be defined in order to re-establish the response to therapy.

AUTHOR INFORMATION

Corresponding Author

*Phone: +33 5 55 43 59 79. E-mail: serge.battu@unilim.fr.

ACKNOWLEDGMENTS

The authors are grateful to Dr. J. Cook-Moreau for corrections in the preparation of this manuscript. The expenses of this work were defrayed in part by the Ministère de l'Education Nationale, de la Recherche et de la Technologie, the Conseil Régional du Limousin, and by the Ligue contre le Cancer (Comité du Limousin). The funders had no role in study design, data collection and analysis, decision to publish, or preparation of the manuscript.

REFERENCES

(1) Ricci-Vitiani, L.; Fabrizi, E.; Palio, E.; De Maria, R. *J. Mol. Med. (Berlin)* **2009**, *87*, 1097−1104.
(2) Fan, X.; Ouyang, N.; Teng, H.; Yao, H. *Int. J. Colorectal Dis.* **2011**, *26*, 1279−1285.
(3) Anderson, E. C.; Hessman, C.; Levin, T. G.; Monroe, M. M.; Wong, M. H. *Cancers (Basel)* **2011**, *3*, 319−339.
(4) Ieta, K.; Tanaka, F.; Haraguchi, N.; Kita, Y.; Sakashita, H.; Mimori, K.; Matsumoto, T.; Inoue, H.; Kuwano, H.; Mori, M. *Ann. Surg. Oncol.* **2008**, *15*, 638−648.
(5) O'Brien, C. A.; Pollett, A.; Gallinger, S.; Dick, J. E. *Nature* **2007**, *445*, 106−110.
(6) Yang, K.; Chen, X. Z.; Zhang, B.; Yang, C.; Chen, H. N.; Chen, Z. X.; Zhou, Z. G.; Chen, J. P.; Hu, J. K. *Int. J. Biol. Markers* **2011**, *26*, 173−180.
(7) Yang, Z. L.; Zheng, Q.; Yan, J.; Pan, Y.; Wang, Z. G. *World J. Gastroenterol.* **2011**, *17*, 932−937.
(8) LaBarge, M. A.; Bissell, M. J. *J. Clin. Invest.* **2008**, *118*, 2021−2024.
(9) Boman, B. M.; Wicha, M. S. *J. Clin. Oncol.* **2008**, *26*, 2795−2799.
(10) Levin, T. G.; Powell, A. E.; Davies, P. S.; Silk, A. D.; Dismuke, A. D.; Anderson, E. C.; Swain, J. R.; Wong, M. H. *Gastroenterology* **2010**, *139*, 2072−2082e5.
(11) Lugli, A.; Iezzi, G.; Hostettler, I.; Muraro, M. G.; Mele, V.; Tornillo, L.; Carafa, V.; Spagnoli, G.; Terracciano, L.; Zlobec, I. *Br. J. Cancer* **2010**, *103*, 382−390.
(12) Munz, M.; Baeuerle, P. A.; Gires, O. *Cancer Res.* **2009**, *69*, 5627−5629.
(13) Yeung, T. M.; Gandhi, S. C.; Wilding, J. L.; Muschel, R.; Bodmer, W. F. *Proc. Natl. Acad. Sci. U.S.A.* **2010**, *107*, 3722−3727.
(14) Caldwell, K. D. *Chem. Sep., Dev. Sel. Pap. Int. Conf. Sep. Sci. Technol., 1st* **1986**, *1*, 41−57.
(15) Reschiglian, P.; Zattoni, A.; Roda, B.; Michelini, E.; Roda, A. *Trends Biotechnol.* **2005**, *23*, 475−483.
(16) Roda, B.; Zattoni, A.; Reschiglian, P.; Moon, M. H.; Mirasoli, M.; Michelini, E.; Roda, A. *Anal. Chim. Acta* **2009**, *635*, 132−143.
(17) Caldwell, K. D.; Cheng, Z. Q.; Hradecky, P.; Giddings, J. C. *Cell Biophys.* **1984**, *6*, 233−251.
(18) Chmelik, J. *J. Chromatogr., A* **1999**, *845*, 285−291.
(19) Giddings, J. C. *Science* **1993**, *260*, 1456−1465.
(20) Martin, M.; Williams, P. S. In *Theoretical Advancement in Chromatography and Related Separation Techniques*; Dondi, F., Guiochon, G., Eds.; Kluwer: Dordrecht, The Netherlands, 1992; Vol. *383*, pp 513−580.
(21) Schure, M. R.; Caldwell, K. D.; Giddings, J. C. *Anal. Chem.* **1986**, *58*, 1509−1516.
(22) Tong, X.; Caldwell, K. D. *J. Chromatogr., B* **1995**, *674*, 39−47.
(23) Williams, P. S.; Lee, S.; Giddings, J. C. *Chem. Eng. Commun.* **1994**, *130*, 143−166.
(24) Battu, S.; Cook-Moreau, J.; Cardot, P. J. P. *J. Liq. Chromatogr. Relat. Technol.* **2002**, *25*, 2193−2210.
(25) Bégaud-Grimaud, G.; Battu, S.; Lazcoz, P.; Castresana, J. S.; Jauberteau, M. O.; Cardot, P. J. P. *Int. J. Oncol.* **2007**, *31*, 883−892.
(26) Bégaud-Grimaud, G.; Battu, S.; Liagre, B.; Beneytout, J. L.; Jauberteau, M. O.; Cardot, P. J. P. *J. Chromatogr., A* **2009**, *1216*, 9125−9133.
(27) Bertrand, J.; Begaud-Grimaud, G.; Bessette, B.; Verdier, M.; Battu, S.; Jauberteau, M. O. *Int. J. Oncol.* **2009**, *34*, 717−727.
(28) Cailleteau, C.; Micallef, L.; Lepage, C.; Cardot, P. J.; Beneytout, J. L.; Liagre, B.; Battu, S. *Anal. Bioanal. Chem.* **2010**, *398*, 1273−1283.
(29) Comte, I.; Battu, S.; Mathonnet, M.; Bessette, B.; Lalloue, F.; Cardot, P.; Ayer-Le Lievre, C. *J. Chromatogr., B* **2006**, *843*, 175−182.
(30) Guglielmi, L.; Battu, S.; Le Bert, M.; Faucher, J. L.; Cardot, P. J. P.; Denizot, Y. *Anal. Chem.* **2004**, *76*, 1580−1585.
(31) Lautrette, C.; Cardot, P. J. P.; Vermot-Desroche, C.; Wijdenes, J.; Jauberteau, M. O.; Battu, S. *J. Chromatogr., B* **2003**, *791*, 149−160.
(32) Leger, D. Y.; Battu, S.; Liagre, B.; Beneytout, J. L.; Cardot, P. J. P. *Anal. Biochem.* **2006**, *355*, 19−28.

(33) Micallef, L.; Battu, S.; Pinon, A.; Cook-Moreau, J.; Cardot, P. J. P.; Delage, C.; Simon, A. *J. Chromatogr., B* **2010**, *878*, 1051−1058.
(34) Bégaud-Grimaud, G.; Battu, S.; Liagre, B.; Léger, D. Y.; Beneytout, J. L.; Cardot, P. J. P. *J. Chromatogr., A* **2006**, *1128*, 194−202.
(35) Bertrand, J.; Liagre, B.; Bégaud-Grimaud, G.; Jauberteau, M. O.; Beneytout, J. L.; Cardot, P. J. P.; Battu, S. *J. Chromatogr., B* **2009**, *877*, 1155−1161.
(36) Plockova, J.; Matulik, F.; Chmelik, J. *J. Chromatogr., A* **2002**, *955*, 95−103.
(37) Zoller, M. *Nat. Rev. Cancer* **2011**, *11*, 254−267.
(38) Ishimoto, T.; Nagano, O.; Yae, T.; Tamada, M.; Motohara, T.; Oshima, H.; Oshima, M.; Ikeda, T.; Asaba, R.; Yagi, H.; Masuko, T.; Shimizu, T.; Ishikawa, T.; Kai, K.; Takahashi, E.; Imamura, Y.; Baba, Y.; Ohmura, M.; Suematsu, M.; Baba, H.; Saya, H. *Cancer Cell* **2011**, *19*, 387−400.
(39) Kuranda, K.; Berthon, C.; Lepretre, F.; Polakowska, R.; Jouy, N.; Quesnel, B. *J. Cell. Biochem.* **2011**, *112*, 1277−1285.
(40) Wilson, A.; Laurenti, E.; Oser, G.; van der Wath, R.; Blanco-Bose, W.; Jaworski, M.; Offner, S.; Dunant, C. F.; Eshkind, L.; Bockamp, E.; Lio, P.; MacDonald, R.; Trumpp, A. *Cell* **2008**, *135*, 1118−1129.